3 Results

The *RASSF1A* tumor suppressor is frequently inactivated in cancer cells by DNA methylation of its CpG island (reviewed by Dammann *et al.*, 2003). However, the mechanisms of transcriptional regulation and epigenetical inactivation of this gene are not identified. *Sp1* protein is a transcription regulator (Dynan and Tjian, 1983), which is associated with promoter protection from *de novo* DNA methylation (Macleod *et al.*, 1994; Brandeis *et al.*, 1994). Four putative *Sp1* binding sites were identified in the *RASSF1A* promoter by *in silicio* analysis. To verify this putative *Sp1* sites, the electro mobility-shift assay (EMSA), luciferase assay, ligation mediated PCR (LM-PCR) and chromatin immunoprecipitation (ChIp) were performed. To identify additional regulatory elements, the *RASSF1A* promoter was analyzed by luciferase assay and *in viv*o footprinting. Further, expressional and epigenetical states of the *RASSF1A* promoter were investigated in consecutive passages of HMECs by quantitative RT-PCR, combined bisulfite restriction analysis (COBRA) and chromatin immunoprecipitation (ChIp) and these data were compared to cells with the active and inactive *RASSF1A* promoter. In summary, in the present study, regulatory elements in the *RASSF1A* promoter were identified and analyzed; the functional relationships between DNA methylation, histone modifications, *Sp1* binding and the *RASSF1A* expression were examined in proliferating HMECs.

3.1 Characterization of regulatory sequences in the *RASSF1A* promoter

In the *RASSF1A* promoter, four putative *Sp1* site were identified by *in silicio* analysis using the Transcription Element Search System (http://www.cbil.upenn.edu/tess). Three putative *Sp1* sites are located in the *RASSF1A* CpG island, which was determined by CpGplot (http://www.ebi.ac.uk). The fourth putative *Sp1* site is located upstream, in the exon 11 of *BLU* gene (Figure 3-1). To analyze mechanism of the *RASSF1A* transcription regulation, four fragments of the *RASSF1A* promoter were cloned in a luciferase reporter vector (*pRL-null*) and verified by *Dual-Luciferase Reporter Assay* system (Figure 3-1). In the Sp1/Ex-pRLnull construct, a 749 bp fragment of the *RASSF1A* promoter including exon 1α and the four putative *Sp1* sites was cloned (Figure 3-1). Sp1/L-pRLnull plasmid contained a 511 bp fragment of the *RASSF1A* promoter including the putative translation start site and four putative *Sp1*

sites (Figure 3-1). For generation of the Su/Ex-pRLnull construct, a 391 bp fragment of the *RASSF1A* promoter containing the three putative *Sp1* sites located in the *RASSF1A* CpG island and exon 1α was used (Figure 3-1). In Su/L-pRLnull construct, a 154 bp fragment of the *RASSF1A* promoter including the putative translation start codon and three putative *Sp1* sites was cloned (Figure 3-1).

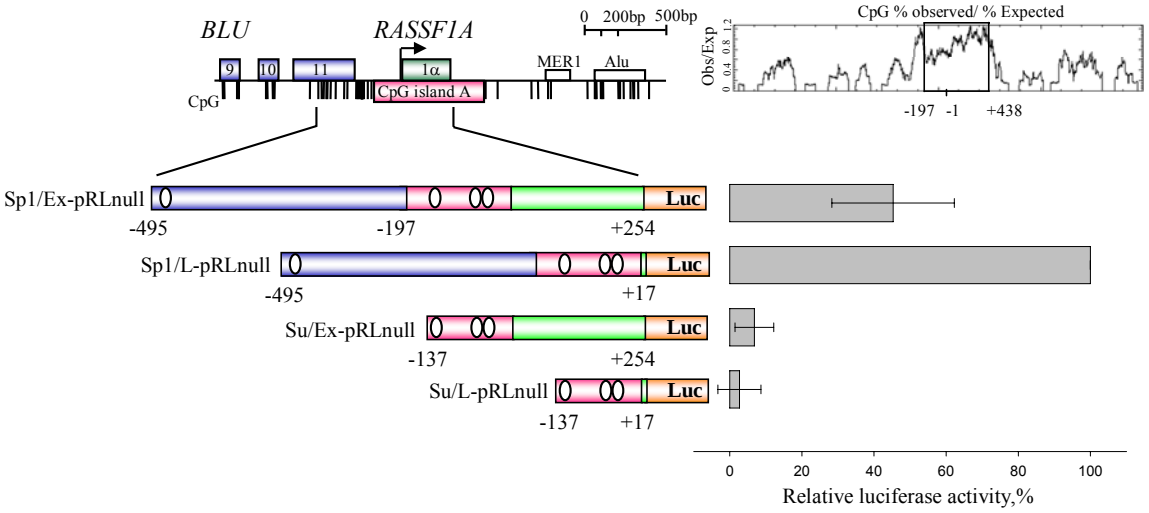

Figure 3-1. Analysis of the *RASSF1A* promoter fragments by *Dual-Luciferase Reporter Assay* system. A map of the *RASSF1A* promoter region is shown. CpG island was determined by CpGplot (http://www.ebi.ac.uk). For further details see Figure 2-1. The four *RASSF1A* fragments (Sp1/EX, Sp1/L, Su/Ex and Su/L) were cloned in the *pRL-null* vector and analyzed by *Dual-Luciferase Reporter Assay* system. The promoter activities of the constructs were compared to the Sp1/L-pRLnull plasmid (=100%). The relative activities of the *RASSF1A* promoter fragments were determined relative to the promoter less *pRL-null* vector (=0%) in three independent assays (standard deviations are indicated). Green and red lines indicate sequences of the exon 1α and the *RASSF1A* CpG island fragment located upstream from the putative translation start, respectively. Blue and yellow lines represent sequences of the putative *RASSF1A* promoter fragment located upstream from CpG island and the *pRL-null* vector, respectively. White dots label the putative *Sp1* sites.

Analysis of luciferase assay data identified that Sp1/L-pRLnull plasmid containing the *RASSF1A* promoter fragment located from -494 up to +17 had the highest transcriptional activity compared to Sp1/Ex-pRLnull, Su/Ex-pRLnull and Su/L-pRLnull in transfected HeLa cells (Figure 3-1). Adding of the *RASSF1A* exon 1α to Sp1/L-pRLnull resulted in two times downregulation of reporter gene activity (Figure 3-1). In Su/Ex and Su/L constructs, absence of the fragment located between -494 and -137 led to 97% and 93% reduction of the promoter activity compared to Sp1/L-pRLnull, respectively (Figure 3-1). Thus, Sp1/L-pRLnull construct had presumably all necessary regulatory elements for transcription.

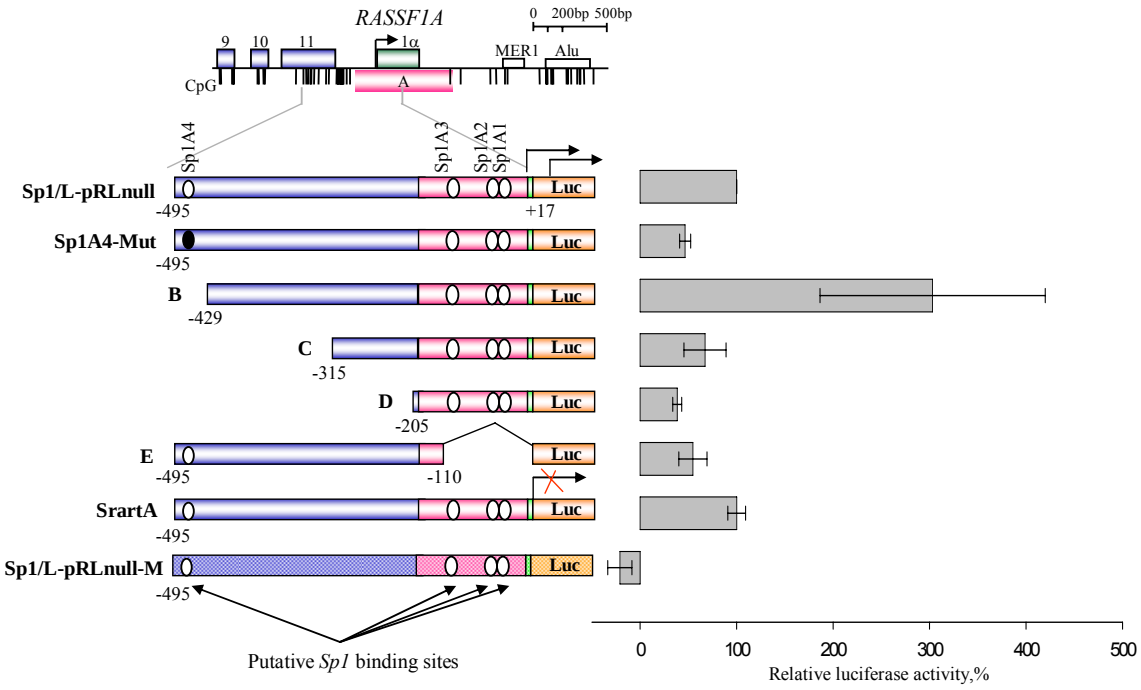

Figure 3-2. Deletion and functional analysis of the *RASSF1A* promoter. A map of the *RASSF1A* promoter region is shown. For further details see Figure 2-1. Using *Dual-Luciferase Reporter Assay* system, the promoter activities of the indicated constructs containing promoter deletions (B, C, D, E) and mutations (StartA and Sp1A4-Mut) were compared to Sp1/L-pRLnull plasmid (=100%). The Sp1/L-pRLnull construct was used for generation analyzed plasmids by mutagenesis. The relative activities of constructs and the *in vitro* methylated plasmid (Sp1/L-pRLnull-M) were determined relative to the promoter less *pRL-null* vector (=0%) in three independent assays (standard deviations are indicated). Black and white dots represent mutated and non-mutated *Sp1* sites, respectively. Green and red lines indicate sequences of the exon 1α and the *RASSF1A* CpG island fragment located upstream from putative translation start, respectively. Blue and yellow lines label sequences of the putative *RASSF1A* promoter fragment located upstream from CpG island and the *pRL-null* vector, respectively.

To identify the localization of the regulatory elements in the *RASSF1A* promoter, several constructs were generated by mutations of the Sp1/L-pRLnull plasmid (Figure 3-2). Mutation of the upstream located *Sp1* site (Sp1A4) resulted in two times downregulation of the transcription activity compared to intact construct (Figure 3-2). In contrast, deletion of a 63 bp fragment containing this *Sp1* site (Sp1A4) resulted in 3 times increasing of the promoter activity compared to intact construct (Figure 3-2). Further deletions of 3' end of the *RASSF1A* promoter fragment led to the downregulation of the luciferase activity compared to intact construct, since the constructs with 180 bp (C) and 290 bp (D) deletions had 23% and 61% decrease in the promoter activity, respectively, compared to intact plasmid (Sp1/L-pRLnull) (Figure 3-2). Deletion of the *RASSF1A* CpG island fragment containing the three putative *Sp1* sites resulted in 45% reduction of promoter activity compared to intact construct (Sp1/L-pRLnull) (Figure 3-2). However, this diminishment is not due to the deletion of

the Kozak consensus, since mutation of ATG to CTG (StartA) showed no significant changes compared to the intact sequence (Sp1/L-pRLnull) (Figure 3-2). *In vitro* methylation of the Sp1/L-pRLnull plasmid (Sp1/L-pRLnull-M) reduced the luciferase expression completely (Figure 3-2).

Shortly, the four putative *Sp1* binding sites located in the *RASSF1A* promoter were analyzed by luciferase assay. According to this analysis, mutation of the upstream putative *Sp1* site (SP1A4) and deletion of the CpG island fragment containing three putative *Sp1* sites led to decreased promoter activities.

3.2 Characterization of regulatory sequences in the *RASSF1C* promoter

Ras associated domain family 1 gene (*RASSF1*) has two main transcript isoforms: *A* and *C* (Dammann *et al.*, 2000). The *RASSF1A* and *RASSF1C* transcriptions initiate at two different CpG islands, which lie 3.5 kb apart. *RASSF1A* is frequently epigenetically inactivated in cancer cells; whereas *RASSF1C* is expressed in cancer cells and its inactivation is detected only in cells containing LOH of this region (reviewed Dammann *et al.*, 2003). The five putative *Sp1* sites were identified upstream from the putative translation start codon of *RASSF1C*. These *Sp1* sites were detected in the *RASSF1C* CpG island, which was determined by CpGplot (http://www.ebi.ac.uk) (Figure 3-3). These sites were the only significant transcription binding positions revealed by *in silicio* analysis of the *RASSF1C* promoter with the Transcription Element Search System (http://www.cbil.upenn.edu/tess). To compare promoter activities of the *RASSF1A* and *RASSF1C* promoters, a 531 bp fragment of the *RASSF1C* CpG island containing the five putative *Sp1* sites was cloned in the *pRL-null* vector (CF-pRLnull) and analyzed by *Dual-Luciferase Reporter Assay* system(Figure 3-3). Analysis of Sp1/L-pRLnull and CF-pRLnull constructs identified that the CF-pRLnull transcription activity was three times higher compared to Sp1/L-pRLnull plasmid (Figure 3-3).

To identify localization of the *RASSF1C* regulatory elements, five constructs with mutations at the putative *Sp1* sites were generated using the CF-pRLnull plasmid (Figure 3-3). Analysis of constructs by the luciferase assay identified that sequential mutation of the four putative *Sp1* sites (Sp1C1, Sp1C2, Sp1C3 and Sp1C4) in the *RASSF1C* promoter resulted in significant reduction of the promoter activity compared to intact construct (CF-pRLnull) (Figure 3-3). Transcription activities of the constructs

with *Sp1* site mutations at position -12 and -52 were 62% and 80% decreased, respectively, compared to intact plasmid (CF-pRLnull) (Figure 3-3). The promoter activity of the construct with mutated *Sp1* site at position –187 was completely abolished and 97% reduction of promoter activity was identified in the construct with the mutated *Sp1* site at position –273 compared to intact plasmid (CF-pRLnull) (Figure 3-3). In contrast, mutation of the *Sp1* site located at –327 had only minor effects on activity of the reporter gene (Figure 3-3).

In summary, the *RASSF1C* promoter fragment containing the five putative *Sp1* sites had three times elevated level of promoter activity compared to the *RASSF1A* promoter fragment containing the four putative *Sp1* sites. In the *RASSF1C* promoter, mutations in the four putative *Sp1* sites led to decrease or inactivation of transcription activity.

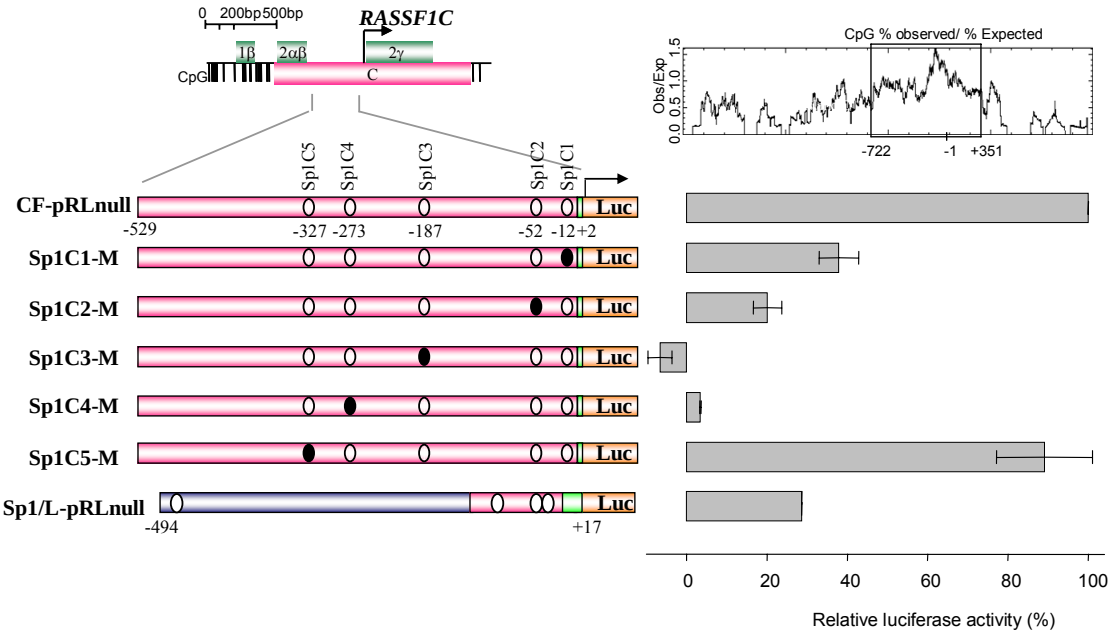

Figure 3-3. Promoter analysis of *RASSF1C* by *Dual-Luciferase Reporter Assay system*. A map of the *RASSF1C* promoter region is shown. The *RASSF1C* CpGs island was determined by CpGplot (http://www.ebi.ac.uk). For further details see Figure 2-1. Using the CF-pRLnull construct, five plasmids were generated by mutagenesis at the putative *Sp1* sites and analyzed by *Dual-Luciferase Reporter Assay* system. The promoter activities of indicated constructs (Sp1C1-M, Sp1C2-M, Sp1C3-M, Sp1C4-M, Sp1C5-M, Sp1/L-pRLnull) were compared to CF-pRLnull promoter activity (=100%). The relative activities of the constructs were determined relative to the promoter less *pRL-null* vector (=0%) in three independent assays (standard deviations are indicated). Green and red lines indicate sequences of the *RASSF1* exons and the CpG island fragments located upstream from translation start, respectively. Blue and yellow lines represent sequences of the putative *RASSF1A* promoter fragment located upstream from CpG island and the *pRL-null* vector, respectively. Black and white dots represent mutated and non-mutated putative *Sp1* sites, respectively.

3.3 Electro mobility-shift assay of the *Sp1* sites located in the *RASSF1A* promoter

To verify the *Sp1* binding to the *RASSF1A* promoter, electro mobility-shift assay (EMSA) was performed (Figure 3-4). For EMSA, eight double stranded oligos were generated. The four of them were 22 bp DNA fragments of the *RASSF1A* promoter containing one from the four putative *Sp1* sites (Sp1A1, Sp1A2, Sp1A3 and Sp1A4). Other four oligos were generated by mutations of the *Sp1* sites (5'GTTCGG) in Sp1A1, Sp1A2, Sp1A3 and Sp1A4 (Sp1A1-m, Sp1A2-m, Sp1A3-m and Sp1A4-m). After incubation of radioactive labelled wildtype oligos with HeLa nuclear protein extract, a shift was detected with Sp1A1, Sp1A2, Sp1A3 and Sp1A4 (Figure 3-4 B, C, D and E). A super-shift was identified when *Sp1* antibodies were added (Figure 3-4 B, C, D and E). In contrast, supershifts were not identified after incubation with *XPA* antibodies (Figure 3-4 B, C, D and E). The cold *Sp1* probes competed for the *Sp1* binding of radioactive labelled oligos (Figure 3-4 B, C, D and E). However, the cold competitors containing the mutated *Sp1* sites (5'GTTCGG) were not able to compete significantly (Figure 3-4 B, C, D and E). Moreover, shifts were found with the methylated in *vitro* oligos containing the *Sp1* sites. In summary, the four *Sp1* sites in the *RASSF1A* promoter were identified according to EMSA analysis.

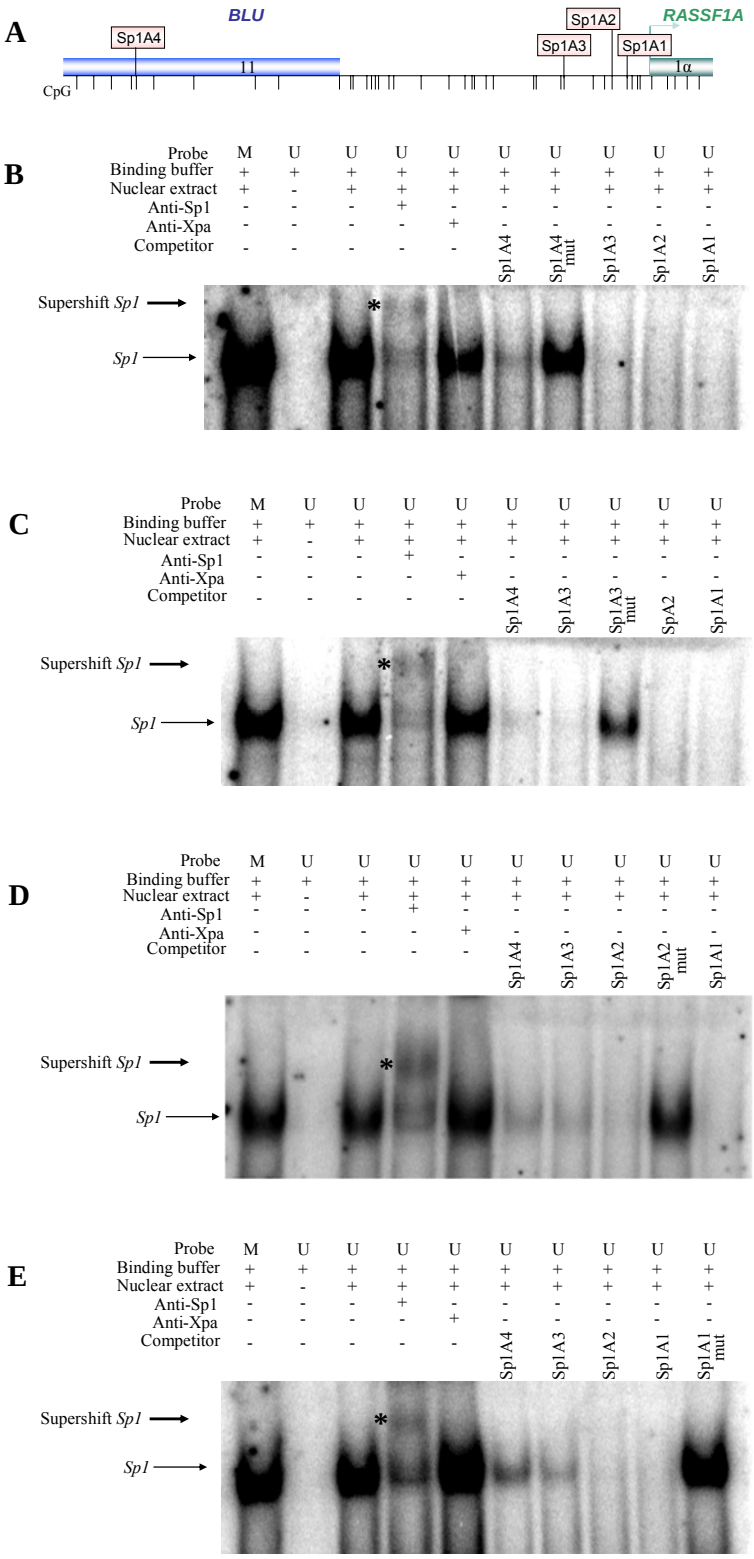

Figure 3-4. EMSA of the four *Sp1* sites located in the *RASSF1A* promoter. A. Map of the *RASSF1A* promoter. Localizations of the four putative *Sp1* sites of the *RASSF1A* promoter, CpGs and exons of *RASSF1A* and *BLU* gene are shown. The arrow indicates the putative start site of the *RASSF1A* translation. **B.** EMSA with labelled Sp1A4 oligo. 22 bp labelled unmethylated (U) and *in vitro* methylated (M) oligos were incubated with HeLa nuclear extract and analyzed by EMSA. Additionally, the oligos were incubated with *Sp1* or *XPA* antibody (supershift is indicated by arrow and asterisk) and competitor oligos. Mutated (mut) competitors were included in the assays. **C.** EMSA with labelled Sp1A3 oligo. **D.** EMSA with labelled Sp1A2 oligo. **E.** EMSA with labelled Sp1A1 oligo.

3.4 Analysis of the *RASSF1A* promoter fragment by *in vivo* footprinting

To verify the *Sp1* binding to the *RASSF1A* promoter, *in vivo* footprinting was performed using the ligation-mediated PCR method (LM-PCR) (Figure 3-5). In the analyzed DNA fragment of the *RASSF1A* promoter, the four hyperreactive Gs were identified at the positions: -481, -468, -461 and -433 relative to the putative translation start codon of *RASSF1A* (Figure 3-5 B and C). The hyperreactive G located at the position -481 belongs to sequence of the upstream *Sp1* site.

Thus, the upstream *Sp1* site (Sp1A4) in the *RASSF1A* promoter was verified by *in vivo* footprinting analysis, EMSA and luciferase assay. An *in vivo* footprinting analysis of *Sp1* sites located in the *RASSF1A* CpG island should be performed in next future.

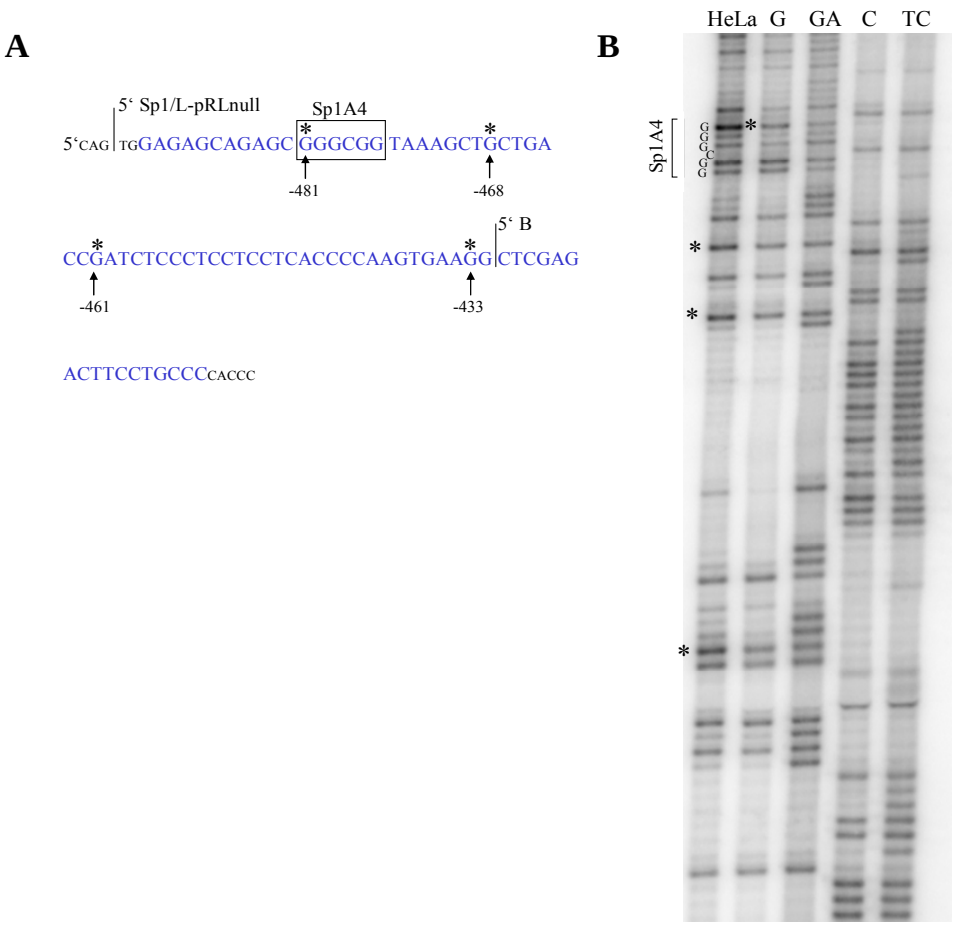

Figure 3-5. ***In vivo*** **footprinting of the** ***RASSF1A*** **promoter fragment. A.** Sequence of the *RASSF1A* promoter fragment. Capital blue letters present the promoter fragment, which was analyzed by LM-PCR. The *Sp1* site is indicated. Hyperreactive Gs in HeLa are marked by asterisks. 5' ends of the *RASSF1A* promoter fragments cloned in the Sp1/L-pRLnull and B vectors are shown. **B.** In *vivo* footprinting of the *RASSF1A* promoter fragment located between -490 and -417 was analyzed by LM-PCR. HeLa lane represents the DNA footprints of HeLa cells treated with DMS *in vivo*. G lane shows footprints of HeLa DNA treated with DMS *in vitro*. Hyperreactive Gs in HeLa and the *Sp1* site are marked. Maxam-Gilbert control sequences are shown (GA, C and TC).

3.5 Transcription patterns of the *RASSF1A* and *RASSF1C* genes in different human tissues.

To investigate the *RASSF1A* and *RASSF1C* expression patterns, expression levels of both genes were analyzed in different human tissues using the *Human MTC panel I* (Clontech). The *RASSF1A* and *RASSF1C* transcriptions were studied in the heart, brain, placenta, lung, liver, skeletal muscle (sk. muscle), kidney and pancreas by real time RT-PCR (Figure 3-6 B, for detail information see supplementary Table 7-1).

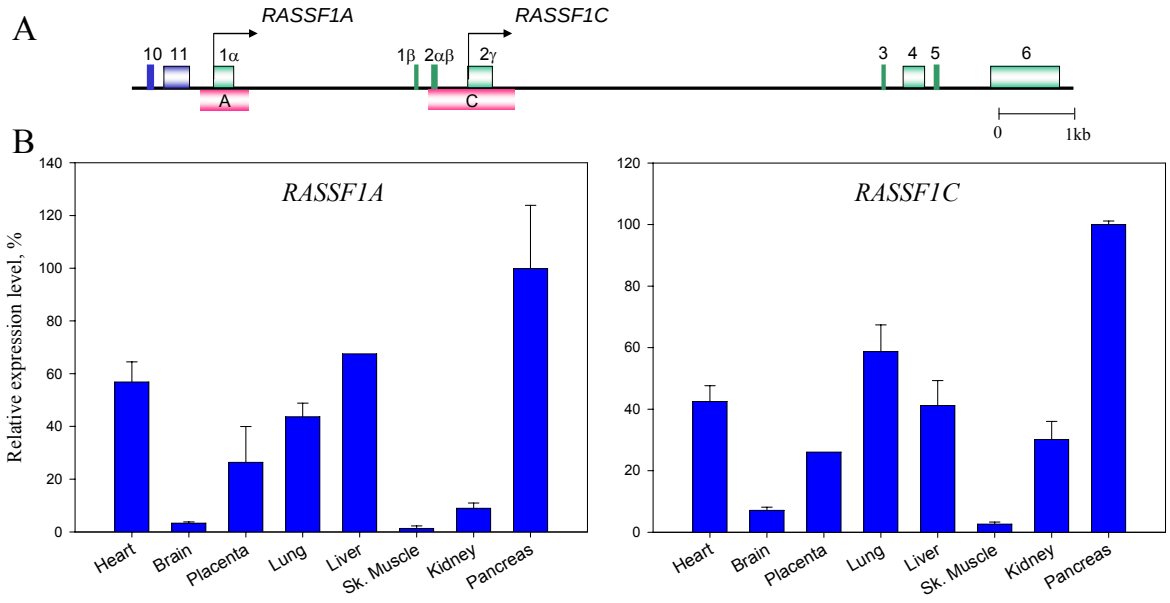

Figure 3-6. Expression of *RASSF1A* and *RASSF1C* in different human tissues. A. A map of the *RASSF1* locus. For further details see Figure 2-1. **B.** The expressions of *RASSF1A* and *RASSF1C* were analyzed in the indicated tissue samples by real time PCR using comparative method of Rotor Gene Software version 4.6. The *RASSF1A* and *RASSF1C* expression levels in different tissues were plotted relative to the transcription levels in the pancreas (=100%). The standard deviations are indicated.

Analysis of the *RASSF1A* and *RASSF1C* expression patterns identified the highest rate of the *RASSF1* transcripts in the pancreas compared to other analyzed tissues (Figure 3-6 B). The expressions of *RASSF1A* and *RASSF1C* in the brain and in the skeletal muscle were between 93% and 98% downregulated compared to the pancreas, respectively (Figure 3-6 B). In the placenta, the *RASSF1A* and *RASSF1C* expression levels were four times reduced compared to the pancreas (Figure 3-6 B). Expressions of *RASSF1* transcripts in the heart, lung and liver were between 42% - 67% of pancreas transcription (Figure 3-6 B). In kidney, *RASSF1A* and *RASSF1C* expressions were 91% and 70% decreased, respectively, compared to the transcription level in the

pancreas (Figure 3-6 B). Thus, similarities in the *RASSF1A* and *RASSF1C* transcription patterns were identified in tissues presented in the *Human MTC panel I*.

3.6 The transcription patterns of *RASSF1A* and *RASSF1C* in different cell lines

To investigate epigenetical inactivation mechanism of the *RASSF1A* promoter, human epithelial cells (HMECs) were analyzed. HMECs have two senescence barriers, which enforce a limited proliferative potential (reviewed by Stampfer and Yaswen, 2003). A first proliferation barrier is a stress or aberrant signaling induced senescence (stasis), which is mediated by *RB*. The second proliferation barrier is termed agonescence and is associated with chromosomal aberrations mediated by critically shortened telomeres.

To analyze the *RASSF1A* expression status, RNA was isolated at various growth phases of five HMEC lines grown for consecutive passages from primary tissue. HMEC-48R and HMEC-184 cell lines were obtained from reduction mammoplasty and provided by Martha Stampfer. HMEC-219 and HMEC-1001 cell lines were purchased from Clonetics and available only at post-stasis stadium. HMEC-219 and HMEC-1001 were sub-cultured until they reached agonescence. HMEC-141 cell line was isolated from normal mammary epithelium-141 (patient 141). HMEC-141 cell line was available at pre-stasis and stasis proliferation phases, since cultivated cells of HMEC-141 did not pass stasis.

The *RASSF1A* and *RASSF1C* expressions were analyzed in HMECs, HF, HeLa, peripheral blood mononuclear cells (PBMC), T47D, ZR75-1, MCF7 and mammary gland (Clontech) by real time RT-PCR (Figure 3-7, for detail information see supplementary Table 7-2 and Table 7-3). Analysis of the *RASSF1A* expression identified the highest transcription activity in PBMC (Figure 3-7 A). High *RASSF1A* expression levels were also observed in HeLa and HF. However, the *RASSF1A* expression in HeLa and HF was two times weaker compared to PBMC (Figure 3-7 A). In the breast cancer cell lines, the *RASSF1A* expression was dramatically reduced or absent and reactivated after four days treatment with 5-Aza-CdR (Figure 3-7 A). Analysis of the *RASSF1A* expression pattern in HMECs identified the *RASSF1A* inactivation during HMECs proliferation (Figure 3-7 A). In the pre-stasis HMECs, 84% reduction of the *RASSF1A* expression was identified compared to HF (Figure 3-7 A). The *RASSF1A* expression level of quiescent mammary gland was comparable to the cells at stasis (Figure 3-7 A).

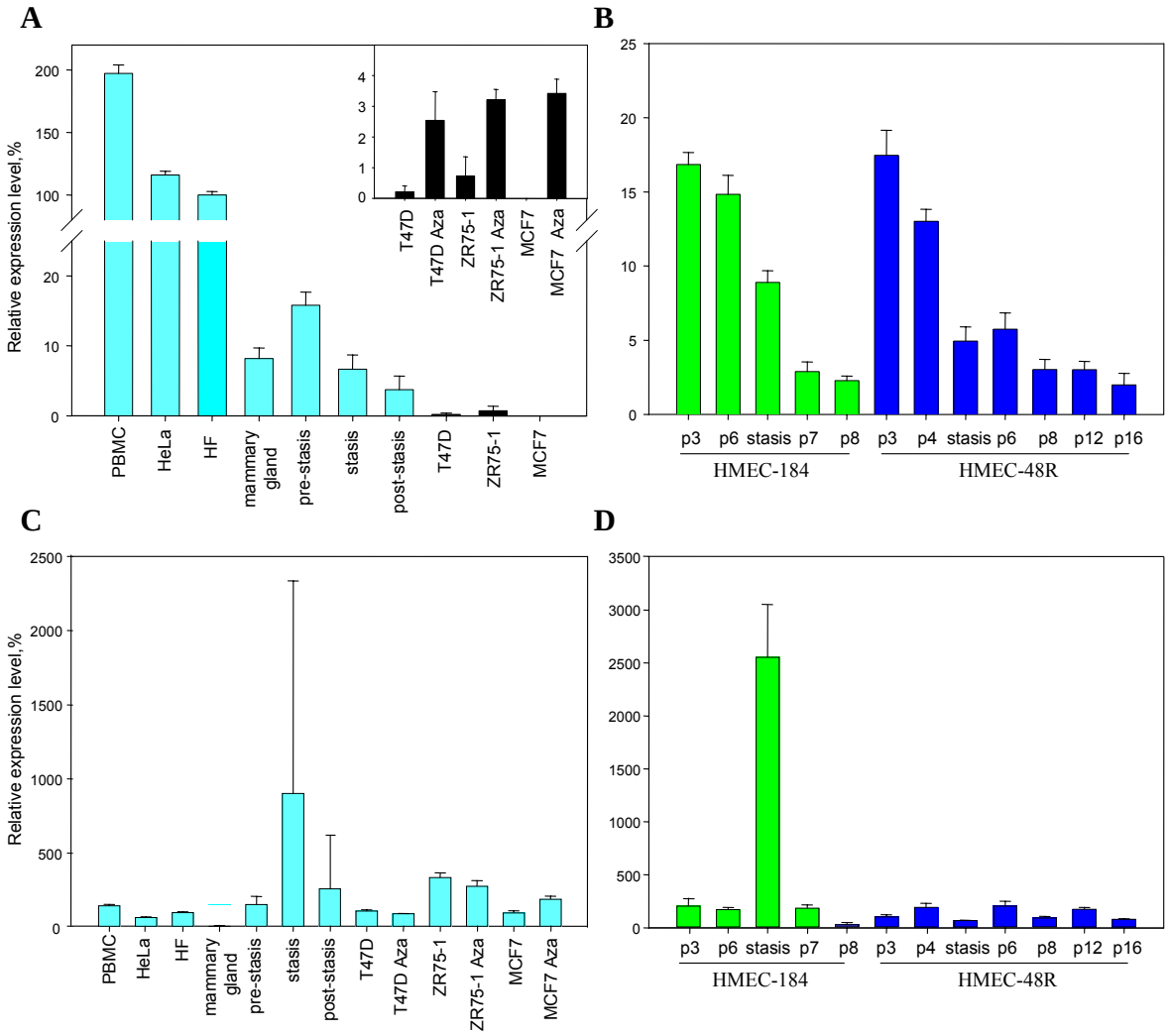

Figure 3-7. Analysis of the *RASSF1A* and *RASSF1C* expressions in the different cell lines. A. The *RASSF1A* expression was analyzed in PBMC, HeLa, HF, mammary gland (Clontech), HMECs (pre-stasis, stasis and post-stasis) and in three breast cancer cell lines (T47D, MCF7 and ZR75-1) by real time RT-PCR using comparative method of the Rotor Gene Software version 4.6. The expression data of three pre-stasis and stasis HMEC isolates (184, 48R, 141) and four post-stasis HMEC (184, 48R, 219 and 1001) were combined. The breast cancer cells were treated for four days with 5-Aza-CdR. The expression levels were plotted relative to transcription level in HF (=100%). The standard deviations are indicated. **B.** The *RASSF1A* expression was analyzed in consecutive passages of HMEC-184 and HMEC-48R. The expression levels were plotted relative to transcription level in HF (=100%). **C.** The *RASSF1C* expression was analyzed in PBMC, HeLa, HF, mammary gland, HMEC (pre-stasis, stasis and post-stasis) and in three breast cancer cell lines (T47D, MCF7 and ZR75-1). The expression data of three pre-stasis and stasis HMEC isolates (184, 48R, 141) and four post-stasis HMEC (184, 48R, 219 and 1001) were combined. The breast cancer cells were treated four days with 5-Aza-CdR. The expression levels were plotted relative to transcription level in HF (=100%). **D.** The *RASSF1C* expression was analyzed in consecutive passages of HMEC-184 and HMEC-48R. The expression levels were plotted relative to transcription level in HF (=100%).

In HMEC-48R cells, 70% and 90% reduction of the *RASSF1A* expression were observed in stasis and in post-stasis (p16) cells, respectively, compared to pre-stasis (p3) (Figure 3-7 B). *RASSF1A* inactivation tendency was identified in the HMEC-184 cells, since 50% and 90% inactivation of the *RASSF1A* transcription were detected in

stasis and post-stasis (p8) cells, respectively, compared to pre-stasis (p3) (Figure 3-7 B). In HMEC-141, HMEC-219 and HMEC-1001, downregulation of the *RASSF1A* expression was detected during proliferation (data are not shown). These data were used to determine the average of the *RASSF1A* expression in pre-stasis, stasis and post-stasis HMECs (Figure 3-7 A). The *RASSF1C* expression was unaffected in analyzed cell lines (Figure 3-7 C). After 5-Aza-CdR treatment of the breast cancer cell lines, no alteration in the *RASSF1C* expression was identified (Figure 3-7 C). Moreover, the *RASSF1C* transcription was not significantly changed in pre-stasis and post-stasis (Figure 3-7 B). However, an upregulation of the *RASSF1C* transcription was observed in HMEC-184 at stasis phase (Figure 3-7 B).

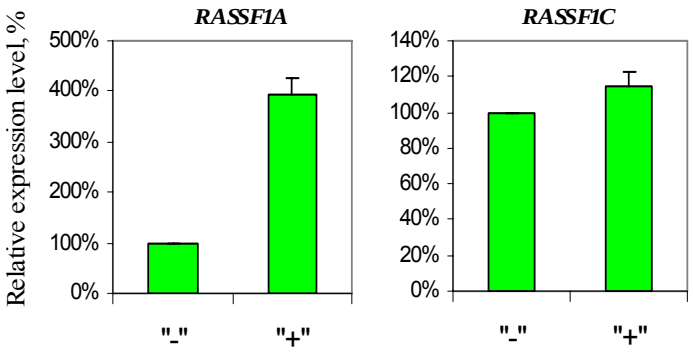

Figure 3-8. The *RASSF1A* and *RASSF1C* expressions in post-stasis HMECs after 5-Aza-CdR treatment. Using real time RT-PCR, the *RASSF1A* and *RASSF1C* expressions were analyzed in HMEC-184 passage 13 cells treated with 5-Aza-CdR for 4 days. The expression levels in the treated cells ("+") were plotted relative to transcription levels in untreated cells ("-") (=100%) using comparative method of the Rotor Gene Software version 4.6. The standard deviations are indicated.

Treatment of HMEC-184 passage 13 (post-stasis) with 5-Aza-CdR for 4 days was performed to investigate the mechanism of the *RASSF1A* inactivation in HMECs (Figure 3-8 and for detail information see Table 7-4). In treated cells, the *RASSF1A* transcription was four times increased compared to the untreated cells, whereas the *RASSF1C* expression was only 10% increased (Figure 3-8). Thus, the *RASSF1A* inactivation during HMEC senescence occurs by epigenetic modifications.

In summary, HMEC senescence is associated with inactivation of the *RASSF1A* transcription. According to Aza-CdR treatment experiments, this inactivation is mediated by DNA methylation.

3.7 Analysis of the epigenetical status of the *p16 INK4* promoter in HMECs

Epigenetical inactivation of tumor suppressor gene, *p16INK4* was already observed in consecutive passages of HMEC-48R and HMEC-184 by Stampfer and colleagues (reviewed by Stampfer and Yaswen, 2003). To compare the *RASSF1A* silencing to *p16INK4* in HMECs, the *p16INK4* methylation pattern and transcription were analyzed in HMEC-141, HMEC-219 and in the breast cancer cell lines by real time RT-PCR and MSP (Figure 3-9, for detail information see supplementary Table 7-5).

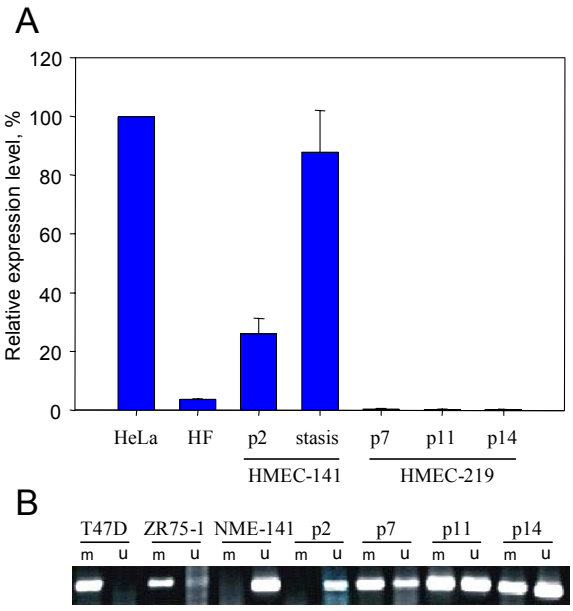

Figure 3-9. The inactivation of *p16 INK4* in HMECs. A. The expression of *p16 INK4* was analyzed in HeLa, HF, HMEC-141 (p2 and p4) and HMEC-219 (p7, p11 and p14) by real time RT-PCR and plotted relative to expression of HeLa (=100%) using comparative method of the Rotor Gene Software version 4.6. The standard deviations are indicated. **B.** The DNA methylation of the *p16 INK4* CpG island was investigated by MSP in NME-141, HMEC-141 and HMEC-219 and in breast cancer cell lines (T47D and ZR75-1). PCR Products of specific primers to methylated (m) and unmethylated DNA (u) were separated on a 2% agarose gel.

In stasis cells (p4) of HMEC-141, three times upregulation of the *p16INK4* transcription was found compared to pre-stasis (p2) using real time RT-PCR (Figure 3-9). Furthermore, the considerably lower expression of *p16INK4* was identified in cells from post-stasis passages of HMEC-219 (Figure 3-9 A). The transcripts of *p16INK4* were completely not detectable in cancer cell lines: A549, T47D, ZR75-1, MCF7 and MDA-MB-231 (data are not shown).

Analysis of the *p16INK4* CpG island identified DNA methylation in post-stasis passages of HMEC-219, whereas in the breast tissue of patient-141 (NME-141) and in HMEC-

141 passage 2, DNA methylation was not detected (Figure 3-9 B). In breast cancer cell lines (T47D and ZR75-1), the $p16^{INK4}$ promoter was completely methylated in all cells, since PCR products of specific primers to the unmethylated $p16^{INK4}$ promoter were not detected (Figure 3-9 B). The upregulation of the $p16^{INK4}$ expression in stasis HMEC-141 and the epigenetical inactivation of $p16^{INK4}$ in post-stasis HMEC-291 confirms the data published by Stampfer and colleagues (Brenner *et al.*, 1998, Olsen *et al.*, 2002).

3.8 Methylation analysis of the *RASSF1* locus

The DNA methylation pattern of the *RASSF1A* locus was investigated by combined bisulfite restriction analysis (COBRA) (Figure 3-10). For COBRA, a 7 kb region flanking the *RASSF1A* CpG island was divided into 12 PCR fragments of 200 to 400 bp lengths containing restriction endonuclease sites for *TaqI*, *HpyCH4IV* or/and *BstUI* (Figure 3-10 A). The ratio of undigested PCR products between restriction (+) and mock (-) digested samples reflects the amount of unmethylated CpG at a specific cutting site (Figure 3-10 B). The *RASSF1A* (RA) and *RASSF1C* (RC) CpG island fragments revealed differences in DNA methylation pattern. In all analyzed cells, the RC fragment was unmethylated (Figure 3-10 B and C). In HF, blood and HeLa, the RA fragment was unmethylated (Figure 3-10 B and C). In contrast, completely DNA methylation of the RA fragment was observed in four breast cancer cell lines (T47D, MDA-MB-231, ZR75-1 and MCF7) and in lung cancer A549 cells (Figure 3-10 B and C). Further, the DNA methylation patterns of the sequences flanking the RA fragment were analyzed. All six segments (D1-D6) located downstream from the putative *RASSF1A* translation start codon were methylated in breast cancer cell lines and A549 cells (Figure 3-10 C). In HeLa and HF, D1 and D2 regions were unmethylated; and D3 and D5 fragments located in different *Alu* elements were methylated at 50% and 100%, respectively (Figure 3-10 C). However, a CpG site (D4) located in a *LINE2* element between the *Alus* was less frequently methylated (25 to 37%) in HeLa and HF (Figure 3-10 C). Three fragments (U2-U4) located upstream from the *RASSF1A* CpG island were frequently methylated in cancer and nonmalignant cells (Figure 3-10 C). In the T47D and MDA-MB-231 cells, DNA hypomethylation of the fragments U4 and U3 was observed (Figure 3-10 B and C). The U1 fragment containing the upstream putative *Sp1* site was less frequently methylated in the *RASSF1A* expressing cells (HeLa, HF, Blood) (0 to 33%) compared to breast cancer cells and A549 cells (>90%)

(Figure 3-10 B and C). Thus, in HF, HeLa and blood, the region containing RA, D1 and D2 fragments was unmethylated in contrast to the breast cancer cell lines and A549 cells, which were characterized by strong DNA methylation of this region. (Figure 3-10 B and C).

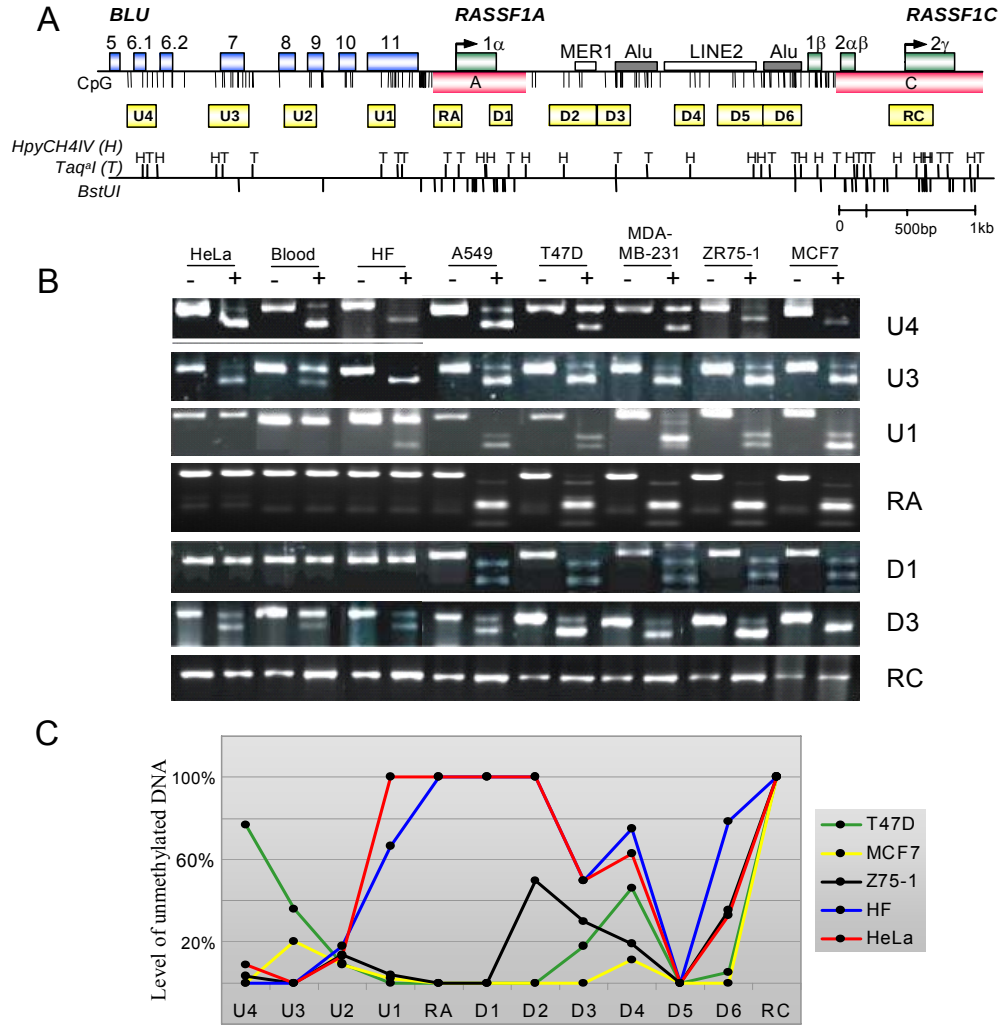

Figure 3-10. DNA methylation analysis of the *RASSF1* locus. A. Map of the *RASSF1* locus. The indicated 12 fragments of the 7 kb locus were analyzed by COBRA. For further details see Figure 2-1. **B.** Representative COBRA analysis of HeLa, blood, HF, A549 and of the breast cancer cell lines (T47D, MDA-MB-231, ZR75-1 and MCF7). PCR products of bisulfite-treated DNA were digested (+) or mock-digested (-) with the appropriate enzymes. **C.** The relative DNA methylation was plotted for the indicated breast cancer cell lines, HF and HeLa.

Furthermore, the DNA methylation patterns of U2, U1, RA, D1 and D2 fragments were investigated in consecutive passages of HMECs. The results of this analysis are presented in Figure 3-11. Using COBRA analysis in HMECs, the strong methylation of the D2 region was observed in contrast to HeLa, HF and blood (Figure 3-10 B and

C, Figure 3-11 B, C and D). In HMECs, DNA methylation was detected in the D1 fragment in contrast to HeLa, HF and blood (Figure 3-10 B and C, Figure 3-11 B, C and D). In HMEC-184, DNA methylation level of the D1 fragment was increasing with cell passages (Figure 3-11 B and D). However, in HMEC-48R, methylation level of the D1 segment was unaffected during cell senescence (Figure 3-11 B and D). In pre-stasis and stasis cells, the RA fragment was unmethylated (Figure 3-11 B, C and D). In this segment, DNA methylation was detected in all post-stasis passages (Figure 3-11 B, C and D). In the U1 region of HMEC-184 passage 8 (p8), level of unmethylated DNA was two times decreased compared to passage 3 (p3) (Figure 3-11 B and D). In HMEC-48R, 14% of unmethylated DNA in U1 region was almost unaffected during senescence (Figure 3-11 C and D). However, the DNA methylation frequency of the U1 fragment was increased and this is indicated by disappearance of partly methylated restriction products during senescence of HMEC-48R and HMEC-184 (Figure 3-11 B, C and D). In HMECs, the DNA methylation of U2 region had the same pattern as in other analyzed cell lines (Figure 3-10 C, Figure 3-11 B, C and D). Similar, COBRA analysis of NME-141, HMEC-141 and HMEC-219 identified spreading the DNA methylation from upstream and downstream into the RA region and *de novo* DNA methylation in the RA fragment (data are not shown).

In summary, the *RASSF1A* expressing cells (HF, HeLa and blood) were characterized by an unmethylated DNA region containing the *RASSF1A* CpG island in contrast to cancer cell lines, which do not express *RASSF1A*. The unmethylated DNA region in the *RASSF1A* CpG island decreased in pre-stasis HMEC compared to HF, HeLa and blood. During HMEC proliferation, spreading of DNA methylation from upstream and downstream into the *RASSF1A* promoter was detected. This was associated with inactivation of the *RASSF1A* expression in consecutive passages of HMECs.

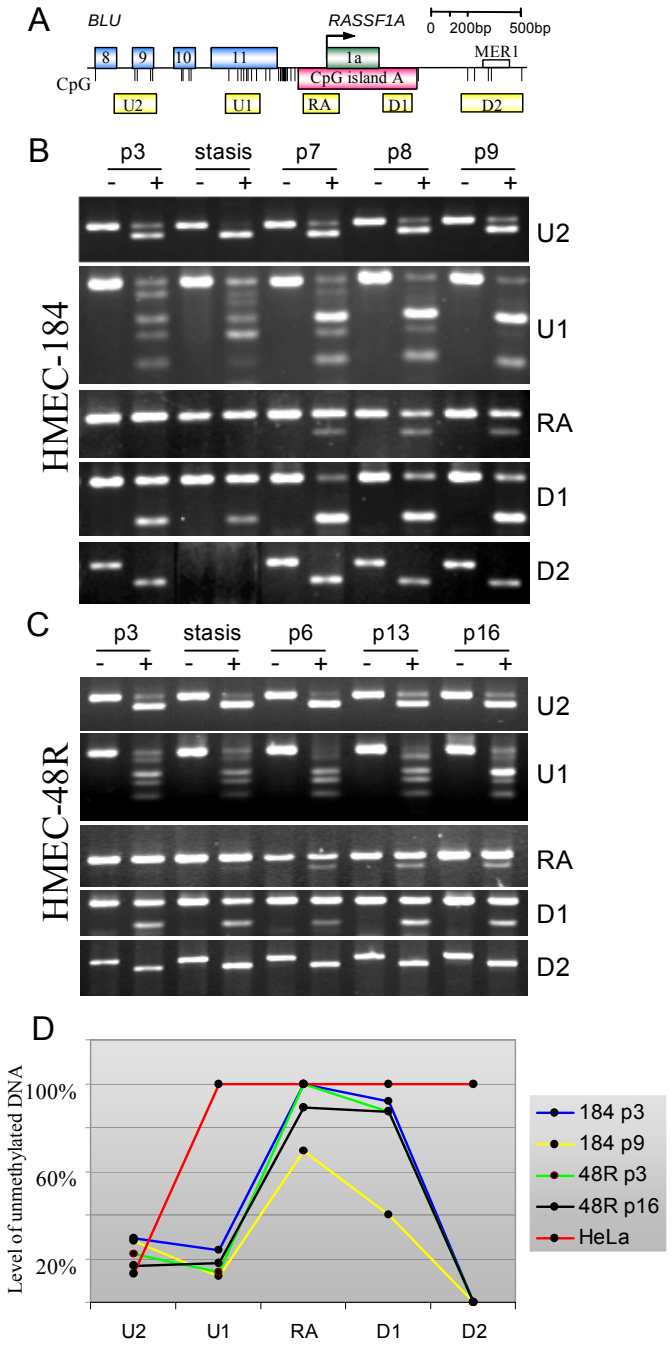

Figure 3-11. Methylation pattern of the *RASSF1A* CpG island and surrounded areas in HMECs. **A.** A map of the *RASSF1* locus. The five indicated DNA fragments of the *RASSF1* locus were analyzed by COBRA. For further details see Figure 2-1. **B.** Representative COBRA analysis of consecutive cell passages of HMEC-184. PCR products of bisulfite-treated DNA were digested (+) or mock-digested (-) with the appropriate enzymes. **C.** Representative COBRA analysis of consecutive cell passages of HMEC-48R. PCR products of bisulfite-treated DNA were digested (+) or mock-digested (-) with the appropriate enzymes. **D.** The relative DNA methylation level was plotted for HMEC-184 passage p3 (p3) and passage 9 (p9), HMEC-48R passage 3 (p3) and passage p16 (p16) and HeLa.

3.9 Sequencing of bisulfite modified DNA of the *RASSF1A* promoter

To analyze DNA methylation pattern of single CpGs in the U1 and RA regions, PCR fragments of bisulfite modified DNA were subcloned and analyzed by sequencing (Figure 3-12). Sixteen and seven CpGs were examined in the RA and U1 fragments obtained from several independent clones, respectively (Figure 3-12). In HF and PBMC, the RA region was completely unmethylated and the U1 fragment was unmethylated in most of the clones. However, methylation of two CpGs located in the *Sp1* binding region at positions -482 and -478 were detected in few clones. In the breast cancer cell line MCF7, almost all analyzed CpGs were methylated in U1 and RA regions (Figure 3-12). Further, the DNA methylation patterns of the U1 and RA fragments were investigated in the consecutive passages of HMECs (Figure 3-12). The RA fragment located in the *RASSF1A* CpG island was unmethylated in NME-141, pre-stasis (p3) and stasis cells of HMEC-184 (Figure 3-12). In this region, methylated CpGs were identified in post-stasis cell (p8) of HMEC-184; however, the DNA methylation density was significantly lower compared to the breast cancer cells (Figure 3-12). The DNA methylation seeds were also identified in the *Sp1* sites located in the RA region. From the eight analyzed U1 sequences of NME-141, only two were unmethylated (Figure 3-12). Interestingly, the unmethylated U1 region was not identified in pre-stasis HMEC-141 cells, which were obtained from NME-141 (Figure 3-12). In HMEC-184, the U1 fragment was frequently methylated. In pre-stasis cells (p3) of HMEC-184, only one from the seven U1 fragments was unmethylated (Figure 3-12). Stasis and post-stasis cells (p8) of HMEC-184 contain only the methylated U1 region (Figure 3-12). Thus, in concordance with the COBRA data, *de novo* DNA methylation of the *RASSF1A* CpG island fragment (RA) located upstream from the *RASSF1A* translation start site was identified during proliferation of HMECs by sequencing of bisulfite modified DNA; and increasing of DNA methylation level in region (U1) containing the upstream *Sp1* site of the *RASSF1A* promoter was observed during senescence of HMECs.

In total, 65 clones containing the U1 fragments with partially methylated sequences from HF, PBMC, blood, MCF7, HMECs and of NME-141 were analyzed (Table 3-1 and data are not shown). In all these clones, DNA methylation of the at least one CpG at positions -482 or -478 was observed (Table 3-1). Both of these CpGs are located in the upstream *Sp1* binding region. Fifty five clones contained both methylated CpGs at these positions and 10 clones had only one methylated CpG at these positions (Table

3-1). Interestingly, DNA methylation occurred preferentially around these two CpGs in most analyzed clones (Table 3-1).

In summary, in pre-stasis cells, the upstream located *Sp1* site was frequently methylated. In the U1 region containing this site, increase of DNA methylation level was observed during senescence of HMECs. In post-stasis HMEC-184 cells, *de novo* DNA methylation occurred in the *RASSF1A* CpG island fragment located upstream from the putative *RASSF1A* translation start site. This methylation level was lower compared to cancer cell line, MCF7.

Table 3-1. Methylation of CpGs at -482 and -478 position in the sequenced clones

Number of clones[1]	CpG methylated at position -482 **OR** -478		CpGs methylated at positions -482 **AND** -478	
	Only one methylated CpG in *Sp1* site [2]	Additionally methylated CpGs [3]	Both methylated CpG in *Sp1* site[4]	Additionally methylated CpGs [5]
65	2/65 (3.08%)	8/65 (12.31%)	6/65 (9.23%)	49/65 (75.38%)
	10/65 (15.3%)		55/65 (84.6%)	

[1]Number of clones with the partially methylated U1 fragments. [2]Number of clones containing only one methylated CpG at positions -482 or -478. [3]Number of clones containing one methylated CpG at position -482 or -478 and methylated CpGs at other positions. [4]Number of clones containing only two methylated CpGs and they are at positions -482 and -478. [5]Number of clones containing methylated CpGs at positions -482 and -478 and methylated CpGs at other positions.

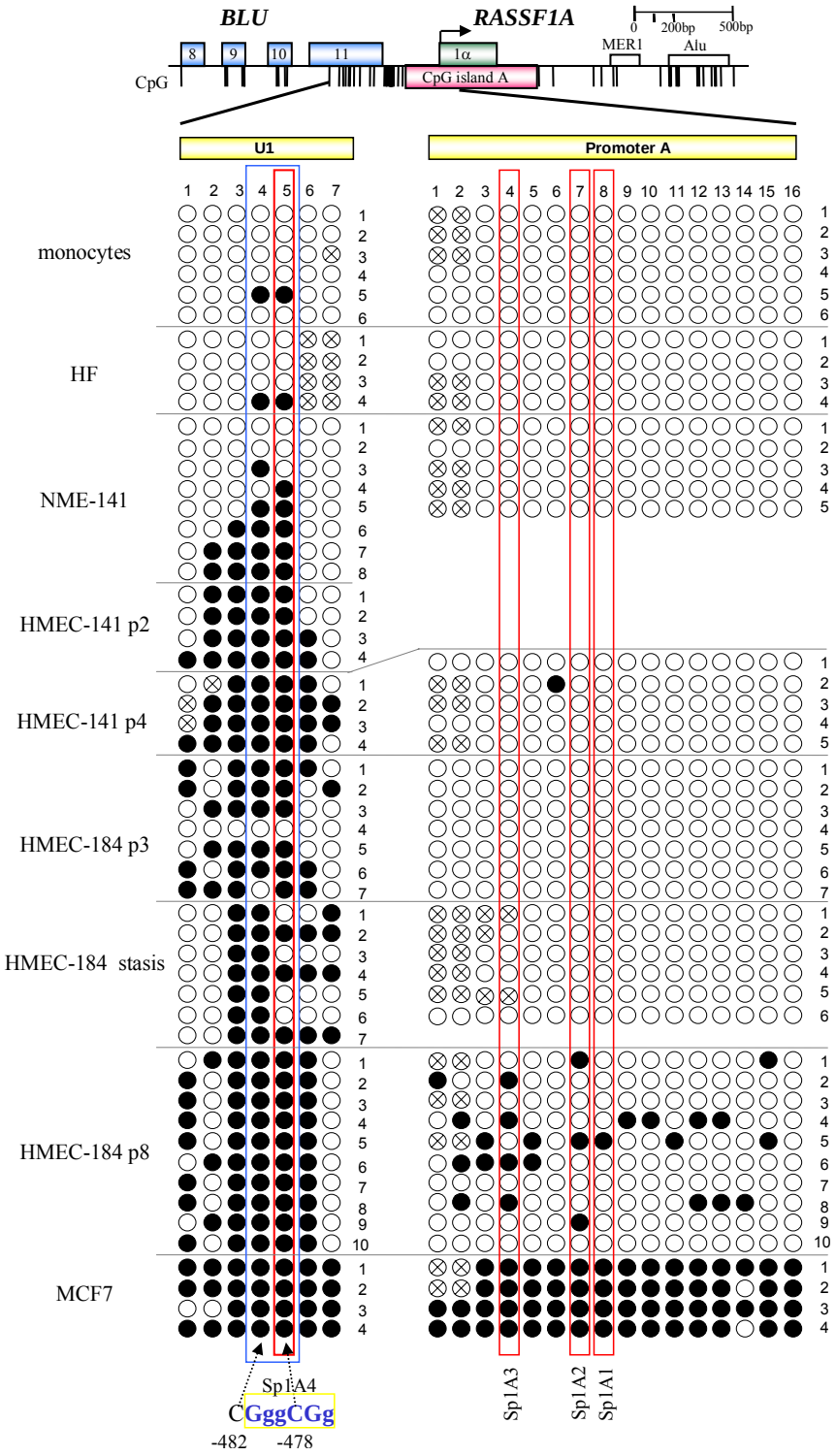

Figure 3-12. Sequencing of bisulfite modified DNA of the *RASSF1A* promoter. A map of the *RASSF1A* promoter region is shown. For further details see Figure 2-1. The two indicated PCR fragments were analyzed by sequencing. Seven and sixteen CpGs of the U1 and RA fragments, respectively, were analyzed in HF, PBMC, NME-141, HMEC-141, HMEC-184 and MCF7. Amplified PCR products were subcloned into the *pGEM-T* vector and several independent clones were sequenced. Black and white dots represent methylated and unmethylated CpGs, respectively. Dots marked with a cross were not analyzable by sequencing. Red and blue outlines indicate the *Sp1* sites and CpG located at positions -482 and -478 relative to the putative *RASSF1*A translation start codon, respectively.

3.10 Histone modifications in the *RASSF1A* and *RASSF1C* promoters

In addition to DNA methylation, distinct chromatin modifications are associated with gene activity (reviewed by Jenuwein and Allis, 2001). Trimethylated histone H3 lysine 9 is a histone modification, which is associated with condensed, inactive chromatin. In contrast, the acetylated histone H3 at lysine 9 and lysine 14 is a hallmark of active chromatin. To investigate histone modifications at the *RASSF1A* and *RASSF1C* promoters, chromatin immunoprecipitation (ChIp) experiments were performed. The A1 and A2 fragments were analyzed in the *RASSF1A* promoter. The A1 fragment contains the upstream *Sp1* binding site. The A2 region is the *RASSF1A* CpG island fragment with the three *Sp1* binding sites. In the *RASSF1C* promoter, the C region containing two *Sp1* sites at positions -187 and -273 was studied. In these three DNA regions, the level of acetylated histone H3 and trimethylated histone H3 lysine 9 were analyzed in HeLa, ZR75-1 and HMEC-184 (Figure 3-13, for detail information see supplementary Table 7-6 and Table 7-7). In HMEC-184, cells from pre-stasis and post-stasis proliferation phases were studied at passage 6 and passage 12, respectively.

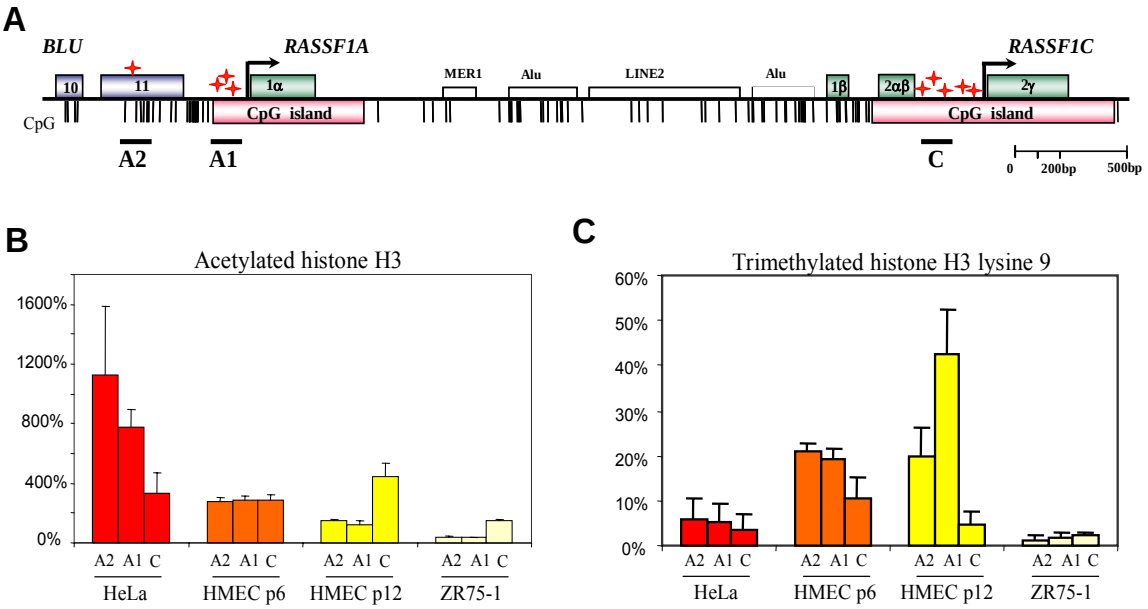

Figure 3-13. Histone modifications in the *RASSF1A* and *RASSF1C* promoters. A. A map of the *RASSF1* locus. For further details see Figure 2-1. Localizations of analyzed fragments are shown. Red stars indicate the *Sp1* sites. **B.** Pattern of acetylated histone H3 was analyzed in HeLa, ZR75-1, HMEC-184 passage 6 (p6) and 12 (p12) by ChIp using real time PCR. Data were verified by comparative method of Rotor Gene Software version 4.6. A "no antibody" probe (=0%) and "input" sample (=100%) were used as controls. The standard deviations are indicated **C.** ChIp assay was performed using antibodies to trimethylated histone H3 lysine 9 in HeLa, ZR75-1 and HMEC-184 passages 6 (p6) and 12 (p12).

Using ChIp, the highest frequency of acetylated histone H3 was detected in the *RASSF1A* promoter in HeLa (Figure 3-13 B). In these cells, level of acetylated histone H3 in the *RASSF1A* promoter was at least two times stronger compared to the *RASSF1C* promoter (Figure 3-13B). In HeLa, the A2 region was characterized by higher frequency of acetylated histone H3 compared to A1 region (Figure 3-13 B). In the *RASSF1C* promoter of pre-stasis HMECs and HeLa, levels of acetylated histone H3 were similar (Figure 3-13 B). The A1 and A2 regions of pre-stasis HMECs were characterized by 2.6 and 4 times decrease of acetylated histone H3 frequencies, respectively, compared to HeLa (Figure 3-13 B). The *RASSF1C* promoter in post-stasis HMECs contained more acetylated histone H3 in contrast to pre-stasis HMECs. In post-stasis HMECs, the *RASSF1A* promoter was associated with two times lower frequency of acetylated histone H3 compared to pre-stasis HMECs (Figure 3-13 B). Thus, level of acetylated histone H3 in the *RASSF1A* promoter decreased during senescence of HMEC-184. In ZR75-1 cells, level of acetylated histone H3 in the *RASSF1C* promoter was about four times higher compared to the *RASSF1A* promoter, which was characterized by the lowest level of acetylated histone H3.

Furthermore, the pattern of trimethylated histone H3 lysine 9 was analyzed (Figure 3-13 C). In ZR75-1 and HeLa, level of this histone modification was similar in the *RASSF1A* and *RASSF1C* promoters (Figure 3-13 C). In pre-stasis and post-stasis HMECs, the *RASSF1A* promoter was characterized by elevated frequency of trimethylated histone H3 lysine 9 compared to the *RASSF1C* promoter (Figure 3-13 C). In pre-stasis HMECs, levels of trimethylated histone H3 lysine 9 were similar in the regions A2 and A1 (Figure 3-13 C). In these cells, the *RASSF1A* promoter and the *RASSF1C* were characterized by elevated frequencies of trimethylated histone H3 lysine 9 compared to HeLa (Figure 3-13 C). During senescence of HMECs, level of trimethylated histone H3 lysine 9 was not changing in the region A2 (Figure 3-13 C). In the *de novo* methylated region A1 of post-stasis HMECs, the highest level of trimethylated histone H3 lysine 9 was identified compared to other analyzed cells (Figure 3-13 C). Thus, elevated frequency of trimethylated histone H3 lysine 9 is associated with *de novo* DNA methylation in the *RASSF1A* promoter in HMEC-184. In the *RASSF1C* promoter of post-stasis HMEC-184 and HeLa, levels of trimethylated histone H3 lysine 9 were similar. During senescence of HMEC, this promoter was associated with a decrease of frequency of trimethylated histone H3 lysine 9 (Figure 3-13 C). In summary, the active transcribing *RASSF1A* and *RASSF1C* promoters are

characterized by elevated frequency of acetylated histone H3. Decreasing of acetylated histone H3 level and increasing of trimethylated histone H3 lysine 9 frequencies were observed in the *RASSF1A* promoter during HMEC senescence. The highest level of trimethylated histone H3 lysine 9 frequency was detected in the *de novo* DNA methylated fragment of the *RASSF1A* CpG island in HMECs.

3.11 The *Sp1* binding to the *RASSF1A* and *RASSF1C* promoters in cell lines

ChIp experiments were performed to analyze *Sp1* binding *in vivo* and to verify EMSA, LM-PCR and luciferase assay data. The *Sp1* binding was studied in the *RASSF1A* (fragments A1 and A2) and *RASSF1C* (fragment C) promoters of HMEC-184 passage 6 and 12, HeLa and ZR75-1 (Figure 3-14).

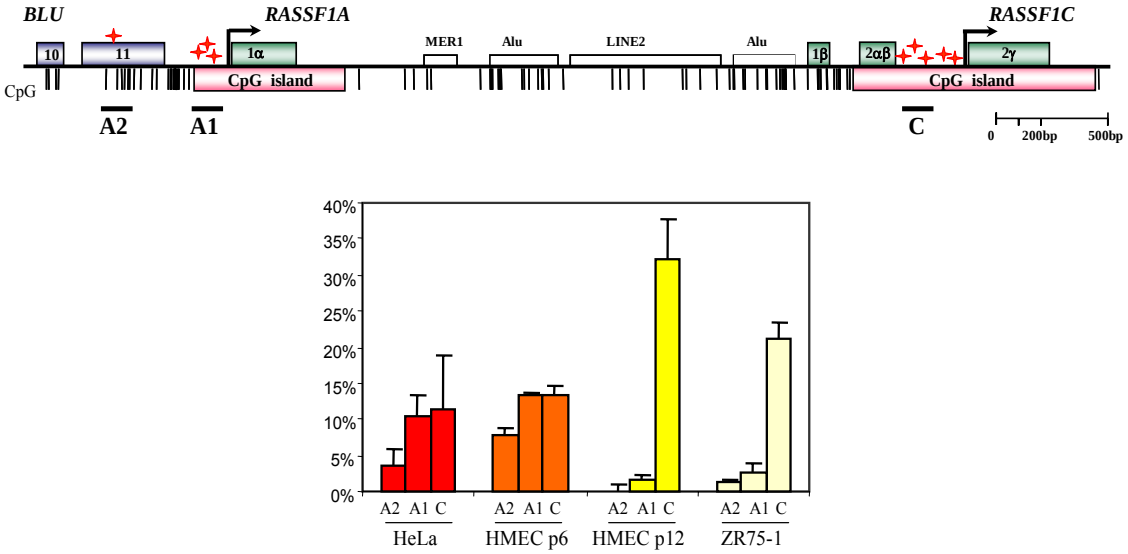

Figure 3-14. *Sp1* binding of the *RASSF1A* and *RASSF1C* promoters. A map of the *RASSF1* locus. For further details see Figure 2-1. Localizations of the analyzed fragments are shown. Red stars indicate the *Sp1* sites. The *Sp1* binding pattern was analyzed in HeLa, HMEC-184 passages 6 (p6) and 12 (p12), ZR75-1 cells using ChIp and real time PCR. Data were verified by comparative method of Rotor Gene Software version 4.6. "No antibody" probe (=0%) and "input" sample (=100%) were used as controls. The standard deviations are indicated.

Analysis of ChIp data indicated strong *Sp1* binding to the *RASSF1C* promoter in all analyzed cell lines (Figure 3-14, for detail information see supplementary Table 7-8). In HeLa and pre-stasis HMECs, the *Sp1* binding had the same pattern and *Sp1* bound with same efficiency both of analyzed CpG islands (A1 and C) (Figure 3-14). In these cells, the *Sp1* binding to the A2 region containing the one *Sp1* binding site was

decreased compared to the fragment A1 with the three *Sp1* sites (Figure 3-14). Interestingly, the methylated *Sp1* site in the A2 region in pre-stasis HMECs was bound by *Sp1* similar as the unmethylated region A2 in HeLa (Figure 3-14). Hence, the *Sp1* binding in the A2 region is not sensitive to DNA methylation. In post-stasis HMECs, repression of *Sp1* binding in the region A2 and strong decreasing of the *Sp1* binding in the region A1 were observed. In post-stasis HMECs, the *Sp1* binding to the *RASSF1C* CpG island (C) was 19 times increased compared to the *RASSF1A* CpG island (A1) and 2.4 times stronger compared to the *RASSF1C* promoter in pre-stasis HMECs (Figure 3-14). Analogously, in ZR75-1, unmethylated *RASSF1C* promoter was bound by *Sp1* at least nine times stronger compared to methylated *RASSF1A* promoter (A2 and A1) (Figure 3-14).

In summary, the *Sp1* binding to the *RASSF1C* promoter was identified in all analyzed cells using ChIp. HeLa cells were characterized by the *Sp1* binding to the *RASSF1A* promoter in contrast to ZR75-1 cells. During HMEC-184 proliferation, occlusion of the *Sp1* binding to the *RASSF1A* promoter was detected. The *Sp1* binding to the upstream located *Sp1* site in the *RASSF1A* promoter does not depend from DNA methylation.